



Design and analysis of SAW pressure sensing element based on IDT/AIN/Mo/diamond multilayered structure

Xiaoxin Ma¹ , Qiang Xiao¹, Yanping Fan², and Xiaojun Ji^{1,*}

¹School of Electronic Information and Electrical Engineering, Shanghai Jiao Tong University, Shanghai 200240, PR China

²School of Optical-Electrical and Computer Engineering, University of Shanghai for Science and Technology, Shanghai 200093, PR China

Received 23 August 2021, Accepted 29 August 2022

Abstract – The multilayer structure of surface acoustic wave sensor is an important development direction of surface acoustic wave devices in recent years. In this paper, the IDT/AIN/Mo/diamond structure of surface acoustic wave pressure sensing element is modeled and simulated. The influence of the thickness of AIN and IDT on pressure coefficient frequency and K^2 were simulated and analyzed. The performance of surface acoustic wave pressure sensing element is compared when the metal layer is Mo, no metal layer and the metal layer is Pt. Finally, the relationship between frequency variation and pressure of the designed multilayer surface acoustic wave pressure sensing element is obtained. This research provides a good guidance for the design of surface acoustic wave pressure sensor.

Keywords: Surface acoustic wave (SAW), Pressure sensing element, Multilayer structure, Finite element method (FEM)

1 Introduction

With the wide application of wireless communication technology and the rapid development of sensor technology, surface acoustic wave (SAW) devices have been widely concerned and applied in academia and industry [1]. SAW devices pursue high electromechanical coupling coefficient (K^2), low insertion loss and high temperature stability. Traditional SAW devices are gradually unable to meet these requirements. In order to improve the performance of SAW devices and expand their applications, multilayer structure SAW devices have received extensive attention in recent years [2–5].

SAW devices with multilayer structure are coated with one or more different dielectric films on the substrate. Compared with traditional SAW devices, dielectric film can change some properties of substrate materials, which brings a new method to develop SAW devices that meet more requirements [6–8]. At present, the research of multilayer structure SAW devices is mainly applied in the field of communication, the application in the field of sensor is rarely reported. The multilayer structure SAW sensing element proposed in this work is made of IDT, AIN, Mo and diamond, the performance of multilayer structure SAW sensing element is studied, and the results provide theoretical guidance for further research [9–11].

AIN thin film is selected as piezoelectric material since it has good piezoelectric properties, it is compatible with integrated circuit (IC) manufacturing process. Considering the electric loss, stability and other factors, Mo was selected as the electrode material. Mo as electrode has high strength and oxidation resistance, good electrical conductivity, long service life, is not easy to corrode and presents other advantages reported in the literature [12–14]. Diamond has high acoustic velocity and high thermal conductivity, so it has a great application prospect in high frequency SAW devices. The advantages of using diamond are various, for example, it hardens the piezoelectric layer, and increases the acoustic velocity of piezoelectric layer [15]. Growing a layer of metal between diamond and AIN has many advantages, metal layer can improve the adhesion of AIN layer and change the propagation characteristics of SAW. Previous studies have shown that there is no reported research on SAW pressure sensing element with AIN/metal layer/diamond multilayer structure. Therefore, the simulation of AIN/Mo/diamond structure SAW pressure sensing element is analyzed in this work.

2 Modeling and simulation

Compared with δ function model and equivalent circuit model, the advantage of finite element method in SAW pressure sensing element design is that the simulation is

*Corresponding author: jxj127@sjtu.edu.cn

more accurate. Considering the periodicity of interdigital transducers (IDT) of SAW pressure sensing element the structure division of finite element simulation, the model can be simplified as a quasi-3D model. Quasi-3D model is a finite element model between 2D model and 3D model, which extends in thickness direction on the basis of 2D model. Quasi-3D model takes into account the advantages of short computing time, saving computing resources of 2D model and high simulation accuracy of 3D model. Five layers existed in this model: IDT can excite surface acoustic wave signals. AlN film is used as piezoelectric material. The metal layer can improve the sensing performance of SAW pressure sensing element. The diamond was employed as support substrate to achieve enlarged phase velocity. The perfectly matched layer (PML) was placed at the bottom of support substrate to avoid wave reflection from the bottom. The thickness of each layer was respectively denoted as h_{IDT} , h_{AlN} , h_{Metal} , h_{Diamond} and h_{PML} .

In this work, multi-physical field simulation software *COMSOL Multiphysics* is used for finite element calculation. Figure 1 shows the quasi-3D periodic finite element model used in this simulation without respecting the actual scaling between elements described after. In this model, the wavelength (λ), corresponding to twice the distance between the electrodes, was 10 μm . The h_{Metal} was 0.1λ , the h_{Diamond} was 7λ . The boundary conditions of the FEM analysis and the material constants of AlN are shown in Tables 1 and 2, respectively.

The electromechanical coupling coefficient K^2 can be estimated by the following formula [17] derived from the equivalent circuit analysis:

$$K^2 = \frac{\pi f_r / 2f_a}{\tan(\pi f_r / 2f_a)}, \quad (1)$$

where f_r is resonance frequency and f_a is anti-resonance frequency of the SAW device. Pressure coefficient of frequency (PCF, see Eq. (2)) reflects the sensitivity of the change of the resonance frequency of SAW sensing element to the pressure. In equation (2), $f_r(P)$ and $f_r(0)$ are the surface acoustic wave resonance frequencies with pressure P and without pressure P respectively.

$$\text{PCF} = \frac{1}{P} \frac{f_r(P) - f_r(0)}{f_r(0)}. \quad (2)$$

The quasi-3D geometry of SAW pressure sensing element is established, and the corresponding materials are added to each part. Solid mechanical field and electrostatic field are coupled. In the physical field of solid mechanics, piezoelectric material is chosen for the part made of AlN, and linear elastic material is chosen for the electrode, the metal layer and the diamond. In the electrostatic physical field, two electrode positions are set as terminal and grounding respectively, and the voltage at terminal position is 1 V (see Fig. 1 and Tab. 1). Finally, the mesh is created and the simulation conditions set in solver. When the model is meshed, one surface of the film layer is mapped first, and then the whole model is meshed by sweeping. The maximum cell size is 1.72E-6m, and the minimum cell size is 1.72E-8m.

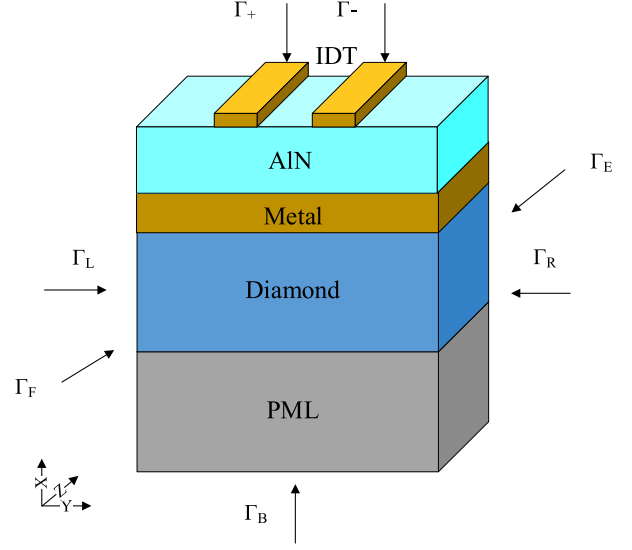


Figure 1. Quasi-3D periodic FEM model used in the simulation (not to scale).

3 Results and discussion

The quasi-3D model of SAW pressure sensing element is simulated and analyzed. The first mode is selected as the main mode. Figure 2 shows the calculated admittance amplitude curve of the first mode of SAW pressure sensing element as a function of frequency for IDT/AlN/Mo/diamond multilayered structure, the resonance frequency is 581.16 MHz. Then the effect of thickness of piezoelectric film AlN on SAW pressure sensing element is analyzed.

To eliminate the effect of electrode thickness, the sensing element structure without IDT is simulated. Figure 3 shows the PCF for the different metal layer materials as a function of normalized AlN thickness. The horizontal coordinate is the thickness of normalized AlN piezoelectric film, and the vertical coordinate is PCF. The relationship between thickness of AlN in piezoelectric film and PCF is compared when the metal layer is Mo, no metal layer and the metal layer is Pt. It can be seen from Figure 3 that PCF increases with the thickness of AlN. When the thickness of normalized AlN reaches 2λ , PCF tends to be stable and does not increase. When the metal layer material is Mo, PCF of the sensing element is higher than that without metal layer structure. The thickness of normalized AlN was 1.5λ when PCF reached the maximum computed value of 68.09 ppm/bar. When metal layer material is Pt, PCF of the sensing element is significantly lower than for the other two cases. Therefore, selecting Mo as a metal layer material can improve the pressure sensitivity of the SAW pressure sensing element in a certain range.

Figure 4 presents the K^2 for different metal layer materials as a function of normalized AlN thickness. As can be seen from the figure, K^2 increases with the thickness of normalized AlN. When the maximum computed value is reached, it decreases gradually. Among them, when the metal layer is Mo, K^2 reaches the maximum computed

Table 1. Boundary conditions of the FEM analysis.

Boundary	Mechanical boundary condition	Electrical boundary condition
Γ_+, Γ_-	Free	$V_{\Gamma_+} = 1 \text{ V}$ $V_{\Gamma_-} = 0 \text{ V}$
Γ_B	Fixed	Ground
Γ_L, Γ_R	Periodical boundary condition	
Γ_F, Γ_E	Periodical boundary condition	

Table 2. Material constants of AlN used in the calculation [16].

Elastic stiffness	c_{11} ($\times 10^{10} \text{ N/m}^2$)	34.5
	c_{12} ($\times 10^{10} \text{ N/m}^2$)	12.5
	c_{13} ($\times 10^{10} \text{ N/m}^2$)	12
	c_{33} ($\times 10^{10} \text{ N/m}^2$)	39.5
	c_{44} ($\times 10^{10} \text{ N/m}^2$)	11.8
	c_{66} ($\times 10^{10} \text{ N/m}^2$)	11
Piezoelectric stress constant	e_{15} (C/m^2)	-0.48
	e_{31} (C/m^2)	-0.45
	e_{33} (C/m^2)	1.55
Dielectric permittivity	ξ_{11}	9
	ξ_{33}	11
Density	ρ (kg/m^3)	3260

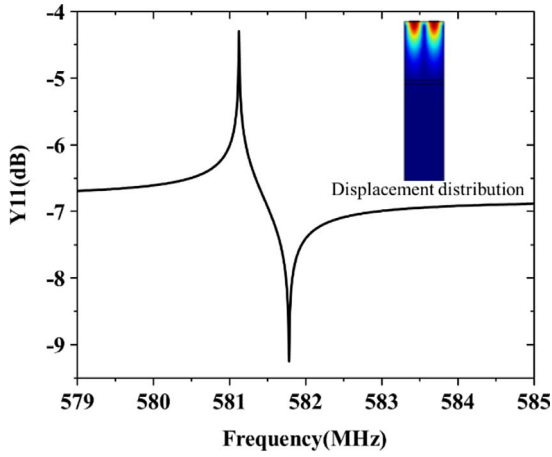


Figure 2. Calculated admittance amplitude (dB) curve.

value of 0.301 when the thickness of normalized AlN is 1.5λ . When the metal layer is Pt, K^2 reaches the maximum value of 0.285 when the normalized thickness of AlN is 2λ . When there is no metal layer, K^2 reaches the maximum computed value of 0.281 when the normalized thickness of AlN is 2.5λ . When the thickness of normalized AlN is 1.5λ , the K^2 of the sensing element with a metal layer Mo structure is significantly larger than that without a metal layer structure.

It can be seen from the above discussion that when the normalized AlN thickness is 1.5λ , PCF and K^2 of the sensing element can reach the maximum computed value when a metal layer made of Mo is used. Therefore, normalized AlN thickness is chosen to be 1.5λ in order to study the effect of IDT thickness on performance of the SAW sensing

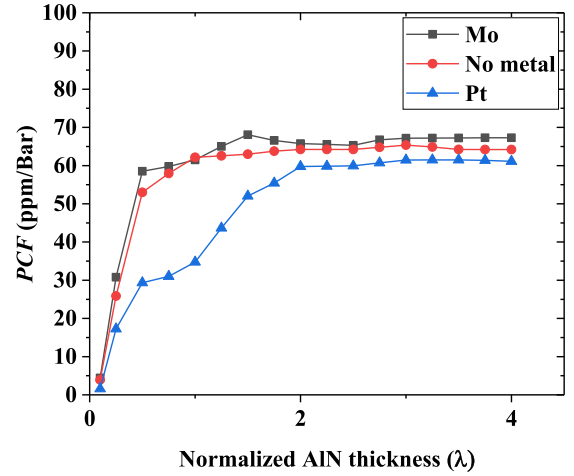


Figure 3. PCF for the different metal layer materials as a function of normalized AlN thickness.

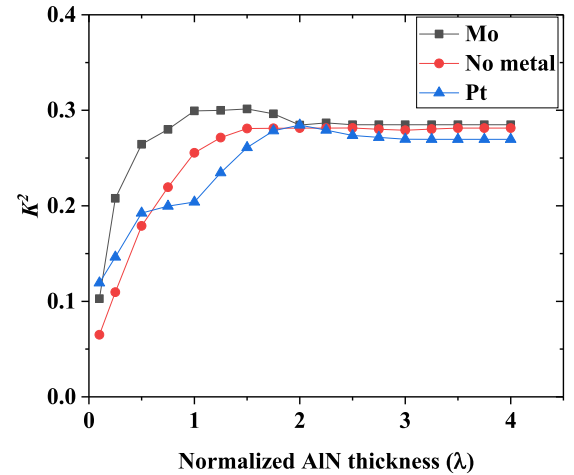


Figure 4. K^2 for the different metal layer materials as a function of normalized AlN thickness.

element. PCF for the different metal layer material as a function of normalized IDT thickness is shown in Figure 5. As can be seen from the figure, PCF tends to decrease with the increase of normalized IDT thickness. PCF of the sensing element with metal layer Mo structure reaches its computed maximum of 63.48 ppm/bar when the normalized IDT thickness is 0.04λ . PCF of the sensing element with metal layer Pt structure reaches its computed maximum of 61.61 ppm/bar when the normalized IDT thickness is 0.03λ . Figure 6 presents K^2 for the different metal layer materials as a function of normalized IDT thickness.

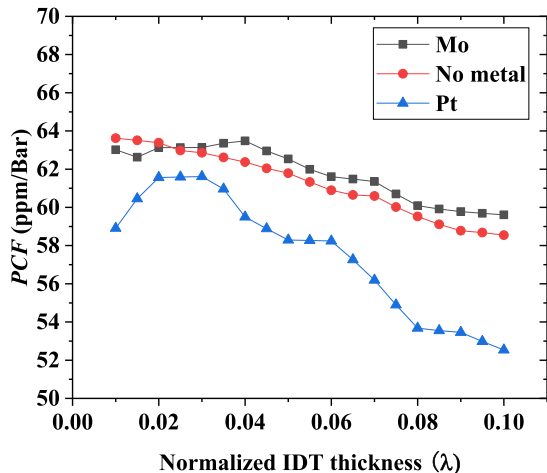


Figure 5. PCF for the different metal layer materials as a function of normalized IDT thickness.

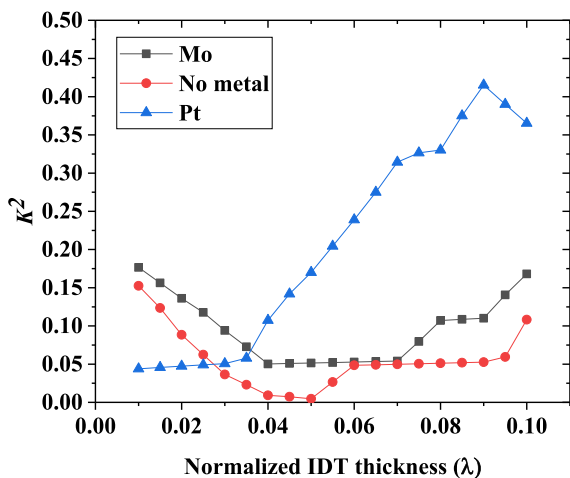


Figure 6. K^2 for the different metal layer materials as a function of normalized IDT thickness.

As the thickness of normalized IDT increases, K^2 of the sensing element with metal layer Pt structure rises continuously, reaching its computed maximum at 0.09λ . K^2 of the sensing element with metal layer Mo structure is slightly higher than that without a metal layer structure. Since K^2 has an impact on the wireless transmission distance of SAW pressure sensor, PCF has a decisive impact on the sensing performance of SAW pressure sensor. Therefore, selecting Mo as metal layer can improve the sensing performance of SAW pressure sensor more effectively.

When the thickness of AlN is 1.5λ , IDT is 0.04λ and Mo is 0.1λ , Figure 7 shows the relationship between frequency variation and pressure of the designed multilayer structure SAW pressure sensing element. The linearity in the range of 0–5 bars is pretty clear, the pressure sensitivity is about -40 kHz/bar. Which meets the design goal of the SAW pressure sensing element. The sensitivity of the traditional SAW pressure sensing element is about 30–35 kHz/bar. In contrast, the pressure sensitivity of the

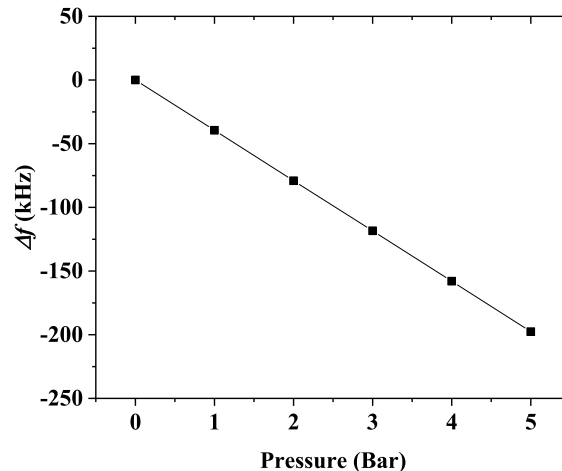


Figure 7. Dependence of Δf on pressure.

multilayer structure SAW pressure sensing element in this work is higher than that of the traditional SAW pressure sensing element.

4 Conclusion

This work investigated the dependence of structural parameters on performance of IDT/AlN/Mo/diamond structure SAW pressure sensing element. The influence of AlN thickness and IDT thickness on PCF and K^2 of the multilayer structure of SAW pressure sensing element is analyzed by using *COMSOL Multiphysics*. Three cases of multilayer structure with metal layer Mo, without metal layer and metal layer Pt are compared and analyzed. The relationship between a frequency variation Δf and a pressure change of the SAW pressure sensing element is simulated and analyzed. The simulation results show that metal layer can enhance the sensing performance of SAW pressure sensing element, which is of reference significance to the design of high-performance SAW pressure sensor.

Conflict of interest

The authors declare that they have no conflict of interest in this work.

Acknowledgments

This work was supported by the National Natural Science Foundation of China (Nos 52075339).

References

1. K.Y. Hashimoto: Surface acoustic wave devices in telecommunications, Springer, Berlin Heidelberg, 2000.
2. F. Seifert, W.E. Bulst, C. Ruppel: Mechanical sensors based on surface acoustic waves. *Sensors & Actuators A: Physical* 44, 3 (1994) 231–239.

3. C. Zhou, Y. Yang, H. Jin, et al.: Surface acoustic wave resonators based on (002) AlN/Pt/diamond/silicon layered structure. *Thin Solid Films* 548 (Dec 2 2013) 425–428.
4. T. Takai, H. Iwamoto, Y. Takamine, et al.: Incredible high performance SAW resonator on novel multi-layered substrate, in 2016 IEEE International Ultrasonics Symposium (IUS), IEEE, 2016.
5. T.M. Reeder, D.E. Cullen: Surface-acoustic-wave pressure and temperature sensors. *Proceedings of the IEEE* 64, 5 (2005) 754–756.
6. M. Kadota, T. Nakao, K. Nishiyama, et al.: Miniature surface acoustic wave devices with excellent temperature stability using high density metal electrodes and SiO₂ film, in International Microwave Symposium Digest, IEEE, 2008.
7. M. Akiyama, K. Kano, A. Teshigahara: Influence of growth temperature and scandium concentration on piezoelectric response of scandium aluminum nitride alloy thin films. *Applied Physics Letters* 95, 16 (2009) 201203.
8. F. Bénédic, M.B. Assouar, P. Kirsch, et al.: Very high frequency SAW devices based on nanocrystalline diamond and aluminum nitride layered structure achieved using e-beam lithography. *Diamond & Related Materials* 17, 4–5 (2008) 804–808.
9. Y. Fan, P. Kong, H. Qi, et al.: A surface acoustic wave response detection method for passive wireless torque sensor. *AIP Advances* 8, 1 (2018) 015321.
10. D. Shaoxu, Q. Mengke, C. Cong, et al.: High-temperature high-sensitivity AlN-on-SOI Lamb wave resonant strain sensor. *AIP Advances* 8, 6 (2018) 065315.
11. H. Xu, S. Dong, W. Xuan, et al.: Flexible surface acoustic wave strain sensor based on single crystalline LiNbO₃ thin film. *Applied Physics Letters* 112, 9 (2018) 093502.
12. S. Chen, Y. Zhang, S. Lin, et al.: Study on the electromechanical coupling coefficient of Rayleigh-type surface acoustic waves in semi-infinite piezoelectrics/non-piezoelectrics superlattices. *Ultrasonics* 54, 2 (2014) 604–608.
13. H. Nakahata, A. Hachigo, K. Higaki, et al.: Theoretical study on SAW characteristics of layered structures including a diamond layer. *IEEE Transactions on Ultrasonics Ferroelectrics & Frequency Control* 42, 3 (2002) 362–375.
14. D.T. Phan, G.S. Chung: FEM modeling SAW humidity sensor based on ZnO/IDTs/AlN/Si structures, in 2011 16th International Solid-State Sensors, Actuators and Microsystems Conference, IEEE, 2011.
15. W.P. Jakubik, M.W. Urbańczyk, S. Kochowski, et al.: Bilayer structure for hydrogen detection in a surface acoustic wave sensor system. *Sensors & Actuators B: Chemical* 82, 2–3 (2002) 265–271.
16. G.S. Chung, D.T. Phan: Finite element modeling of surface acoustic waves in piezoelectric thin films. *Journal- Korean Physical Society* 57, 3 (2010) 446–450.
17. T. Li, H. Hong, X. Gang, et al.: Pressure and temperature micro-sensor based on surface acoustic wave in TPMS, InTech, 2010.

Cite this article as: Ma X. Xiao Q. Fan Y. & Ji X. 2022. Design and analysis of SAW pressure sensing element based on IDT/AlN/Mo/diamond multilayered structure. *Acta Acustica*, 6, 38.